first year of life. Her affected father also had attacks with fever and abdominal pain between the ages of 5 and 12 years.

Because of the similarity of their symptoms to CAPS, their disease was designated as FCAS2 (OMIM #611762). Through an extensive search for mutations in NLR family molecules, heterozygous nonsense or insertion mutations in the *NLRP12* gene have been identified in each family.[5] A base-pair insertion within the donor splice site of intron 3 activates a cryptic donor splice site, resulting in a frame shift and a premature termination. As NLRP12 has been shown to be a negative regulator of nuclear factor (NF)-κB signaling and such an inhibitory effect was actually impaired by these mutations, their heterozygosity seems to cause haploinsufficiency in patients.[45]

PLAID

Three unrelated families with autosomal dominantly inherited atypical cold urticaria were first reported in 2009.[46] As a characteristic feature, water evaporation seems to be the most effective stimulus, which is occasionally induced by tears flowing down the cheeks or warm water on the skin exposed to room temperature. Accordingly, the patients show a negative cold-stimulation test using ice cubes, whereas urticarial rashes appear after direct contact of ice to the skin followed by rewarming to room temperature. Outdoor cold air also induces urticarial rash over unprotected areas. All patients experienced pruritus and erythema, whereas angioedema was experienced by less than half of the cases. Reactions are local rather than generalized, are not accompanied by systemic complications, and usually resolve within 30 minutes. Of note, ingestion of cold foods or beverages caused oropharyngeal swelling in some cases. Most patients develop the symptoms before 6 months of age and sustain them for life, although their severity usually improves after 30 years of age. The disease has been designated as familial atypical cold urticaria (FACU) or FCAS3 (OMIM #614468), which is clearly distinguished from FCAS by the absence of systemic involvement.

In 2012, immunologic abnormalities were added to their clinical features. These abnormalities include recurrent infections associated with low immunoglobulin (Ig)A and IgM, and high IgE levels in the serum, decreased circulating B cells and natural killer (NK) cells, and development of autoantibodies or autoimmune diseases and granulomatous skin lesions.[6] Through linkage analysis, 3 different heterozygous deletions in the *PLCG2* gene have been identified as responsible, and the disease has been designated as PLAID. Phospholipase C (PLC) family enzymes hydrolyze membranous phospholipids and generate diacylglycerols and inositol triphosphate to activate calcium influx. Among them, PLCγ2 is expressed in B, NK, and mast cells, and involves signaling through various receptor tyrosine kinases. All 3 deletions are included in the C-terminal Src-homology-2 (SH2) domain with an autoinhibitory role, and lack of this domain has been shown to increase the phospholipase activity of PLCγ2. The downstream functions of the immune cells, however, were mostly decreased, probably as a result of chronic signaling. By contrast, mast cells with mutant *PLCG2* showed spontaneous degranulation at 20°C, probably responsible for cold urticaria.[6]

Almost simultaneously, familial cases showing recurrent blistering skin lesions with inflammatory lesions of the joints, eyes, and gastrointestinal tract were reported.[7] Their skin lesions resembled epidermolysis bullosa in infancy, but progressed to erythematous plaques with vesiculopustules, which worsened with heat and sun exposure. These patients also showed mild deficiency of humoral immunity causing recurrent sinopulmonary infections, without circulating autoantibodies. Through whole exome sequencing, a heterozygous gain-of-function missense mutation in the *PLCG2*

Table 4
Hereditary diseases with cold-induced urticaria

		Episodic Symptoms	Sustained/Progressive Symptoms
CAPS	FCAS	Urticarial rash, arthralgia, myalgia, chills, fever, swelling of the extremities	Renal amyloidosis
	MWS	Urticarial rash, arthralgia, chills, fever	Sensorineural deafness, renal amyloidosis
	CINCA	Fever	Rash, arthritis, chronic meningitis, visual defect, deafness, growth retardation, renal amyloidosis
NAPS12 (FCAS2)		Fever, arthralgia, myalgia, urticaria, abdominal pain, aphthous ulcers, lymphadenopathy	Sensorineural deafness
PLAID (FCAS3)		Urticaria induced by evaporative cooling, sinopulmonary infections	Serum low immunoglobulin (Ig)M and IgA levels, high IgE levels, decreased B and NK cells, granulomata, antinuclear antibodies

gene has been identified as being responsible.[7] Despite some distinctive clinical and genetic features, the diseases in this family and the families with PLAID possibly form a distinct type of hereditary autoinflammatory syndrome with immunodeficiency. The clinical features of hereditary diseases with cold-induced urticaria are summarized in Table 4.

OTHER GENETICALLY UNDEFINED HEREDITARY URTICARIA

On searching the OMIM database, several disorders with distinct OMIM numbers remain to be genetically defined. Aquagenic urticaria (OMIM 191850) is characterized by urticaria induced by contact with water but not by heat or cold, and its familial occurrence was reported in 1979.[47] Familial cases with delayed heat urticaria were reported as familial localized heat urticaria (OMIM 191950),[48] in which the lesions were limited to the areas of contact with heat and were completely inhibited by local lidocaine pretreatment. Another 2 forms of familial physical urticaria, dermodistortive urticaria (OMIM 125630) and familial dermographism (OMIM 125635), are also registered.[49,50] The former is induced by repetitive vibratory or stretching stimulation, whereas the latter is defined by wheal formation on the skin after a single stroke with moderate pressure.

SUMMARY

Hereditary disorders presenting with urticaria are not common and may not be encountered by most physicians. However, without the correct knowledge they can be easily missed or misdiagnosed. With proper diagnosis and understanding of the genetic cause and consequent pathogenesis, disease-specific essential therapeutic regimens can be offered. Recent discovery of the genetic origins of rare cases with distinct hereditary cold urticaria encourages the examination of more cases. As technology in genetic analysis progresses rapidly, further insights into undefined hereditary urticaria will emerge in the near future. The knowledge obtained promises to lead to the development of novel therapeutics.

REFERENCES

1. Hide M, Hiragun T. Japanese guidelines for diagnosis and treatment of urticaria in comparison with other countries. Allergol Int 2012;61:517–27.
2. Fuller SJ. New insights into the pathogenesis, diagnosis, and management of mastocytosis. Hematol Oncol Clin North Am 2012;26:1143–68.
3. Cicardi M, Johnston DT. Hereditary and acquired complement component 1 esterase inhibitor deficiency: a review for the hematologist. Acta Haematol 2012;127:208–20.
4. Yu JR, Leslie KS. Cryopyrin-associated periodic syndrome: an update on diagnosis and treatment response. Curr Allergy Asthma Rep 2011;22:12–20.
5. Jeru I, Duquesnoy P, Fernandes-Alnemri T, et al. Mutations in NALP12 cause hereditary periodic fever syndromes. Proc Natl Acad Sci U S A 2008;105:1614–9.
6. Ombrello MJ, Remmers EF, Sun G, et al. Cold urticaria, immunodeficiency, and autoimmunity related to PLCG2 deletions. N Engl J Med 2012;366:330–8.
7. Zhou Q, Lee GS, Brady J, et al. A hypermorphic missense mutation in PLCG2, encoding phospholipase Cγ2, causes a dominantly inherited autoinflammatory disease with immunodeficiency. Am J Hum Genet 2012;91:713–20.
8. Kettelhut BV, Metcalfe DD. Pediatric mastocytosis. J Invest Dermatol 1991;96: 15S–8S.
9. Middelkamp Hup MA, Heide R, Tank B, et al. Comparison of mastocytosis with onset in children and adults. J Eur Acad Dermatol Venereol 2002;16:115–20.
10. Topar G, Staudacher C, Geisen F, et al. Urticaria pigmentosa: a clinical, hematopathologic, and serologic study of 30 adults. Am J Clin Pathol 1998;109: 279–85.
11. Wolff K, Komr M, Petzelbauer P. Clinical and histopathological aspects of cutaneous mastocytosis. Leuk Res 2001;25:519–28.
12. Golitz LE, Weston WL, Lane AT. Bullous mastocytosis: diffuse cutaneous mastocytosis with extensive blisters mimicking scalded skin syndrome or erythema multiforme. Pediatr Dermatol 1984;1:288–94.
13. Horny HP, Parwaresch MR, Lennert K. Bone marrow findings in systemic mastocytosis. Hum Pathol 1985;16:808–14.
14. Longley BJ, Metcalfe DD, Tharp M, et al. Activating and dominant inactivating c-KIT catalytic domain mutations in distinct clinical forms of human mastocytosis. Proc Natl Acad Sci U S A 1999;96:1609–14.
15. Bodemer C, Hermine O, Palmerini F, et al. Pediatric mastocytosis is a clonal disease associated with D816V and other activating c-KIT mutations. J Invest Dermatol 2010;130:804–15.
16. Garcia-Montero AC, Jara-Acevedo M, Teodosio C, et al. KIT mutation in mast cells and other bone marrow hematopoietic cell lineages in systemic mast cell disorders: a prospective study of the Spanish Network on Mastocytosis (REMA) in a series of 113 patients. Blood 2006;108:2366–72.
17. Fett NM, Teng J, Longley BJ. Familial urticarial pigmentosa: report of a family and review of the role of KIT mutations. Am J Dermatopathol 2013;35:113–6.
18. Gleixner KV, Mayerhofer M, Ceyny-Reiterer S, et al. KIT-D816V-independent oncogenic signaling in neoplastic cells in systemic mastocytosis: role of Lyn and Btk activation and disruption by dasatinib and bosutinib. Blood 2011;118: 1885–98.
19. Yanagihori H, Oyama N, Nakamura K, et al. c-KIT Mutations in patients with childhood-onset mastocytosis and genotype-phenotype correlation. J Mol Diagn 2005;7:252–7.

20. Shaw JM. Genetic aspects of urticaria pigmentosa. Arch Dermatol 1968;97: 137–8.
21. Wasag B, Niedoszytko M, Piskorz A, et al. Novel, activating KIT-N822I mutation in familial cutaneous mastocytosis. Exp Hematol 2011;39:859–65.
22. Quincke HI. Uber akutes umschriebenes Hautoderm. Monatsh Prakt Derm 1882;1:129–31.
23. Donaldson VH, Evans RR. A biochemical abnormality in hereditary angioneurotic edema: absence of serum inhibitor of C'1-esterase. Am J Med 1963;35:37–44.
24. Lumry WR, Castaldo AJ, Vernon MK, et al. The humanistic burden of hereditary angioedema: impact on health-related quality of life, productivity, and depression. Allergy Asthma Proc 2010;31:407–14.
25. Nzeako UC, Frigas E, Tremaine WJ. Hereditary angioedema: a broad review for clinicians. Arch Intern Med 2001;161:2417–29.
26. Bork K, Barnstedt SE, Koch P, et al. Hereditary angioedema with normal C1-inhibitor activity in woman. Lancet 2000;356:213–7.
27. Dewald G, Bork K. Missense mutations in the coagulation factor XII (Hageman factor) gene in hereditary angioedema with normal C1 inhibitor. Biochem Biophys Res Commun 2006;343:1286–9.
28. Cichon S, Martin L, Hennies HC, et al. Increased activity of coagulation factor XII (Hageman factor) causes hereditary angioedema type III. Am J Hum Genet 2006;79:1098–104.
29. Nussberger J, Cugno M, Amstutz C, et al. Plasma bradykinin in angio-oedema. Lancet 1998;351:1693–7.
30. Bowen T, Cicardi M, Farkas H, et al. 2010 international consensus algorithm for the diagnosis, therapy and management of hereditary angioedema. Allergy Asthma Clin Immunol 2010;6:24.
31. Kile RL, Rusk HA. A case of cold urticaria with unusual family history. JAMA 1940;114:1067–8.
32. Muckle TJ, Wells M. Urticaria, deafness and amyloidosis: a new heredo-familial syndrome. Q J Med 1962;31:235–48.
33. Hoffman HM, Mueller JL, Broide DH, et al. Mutation of a new gene encoding a putative pyrin-like protein causes familial cold autoinflammatory syndrome and Muckle-Wells syndrome. Nat Genet 2001;29:301–5.
34. Kastner DL, O'Shea JJ. A fever gene comes in from the cold. Nat Genet 2001; 29:241–2.
35. Feldmann J, Prieur AM, Quartier P, et al. Chronic infantile neurological cutaneous and articular syndrome is caused by mutations in *CIAS1*, a gene highly expressed in polymorphonuclear cells and chondrocytes. Am J Hum Genet 2002;71:198–203.
36. Aksentijevich I, Nowak M, Mallah M, et al. De novo CIAS1 mutations, cytokine activation, and evidence for genetic heterogeneity in patients with neonatal-onset multisystem inflammatory disease (NOMID): a new member of the expanding family of pyrin-associated autoinflammatory diseases. Arthritis Rheum 2002;46:3340–8.
37. Arostegui JI, Aldea A, Modesto C, et al. Clinical and genetic heterogeneity among Spanish patients with recurrent autoinflammatory syndromes associated with the CIAS1/PYPAF1/NALP3 gene. Arthritis Rheum 2004;50:4045–50.
38. Tanaka N, Izawa K, Saito MK, et al. High incidence of NLRP3 somatic mosaicism in patients with chronic infantile neurologic, cutaneous, articular syndrome: results of an international multicenter collaborative study. Arthritis Rheum 2011; 63:3625–32.

39. Kersse K, Bertrand MJ, Lamkanfi M, et al. NOD-like receptors and the innate immune system: coping with danger, damage and death. Cytokine Growth Factor Rev 2011;22:257–76.
40. McDermott MF, Tschopp J. From inflammasomes to fevers, crystals and hypertension: how basic research explains inflammatory diseases. Trends Mol Med 2007;13:381–8.
41. Nakamura Y, Kambe N, Saito M, et al. Mast cells mediate neutrophil recruitment and vascular leakage through the NLRP3 inflammasome in histamine-independent urticaria. J Exp Med 2009;206:1037–46.
42. Hoffman HM, Rosengren S, Boyle DL, et al. Prevention of cold-associated acute inflammation in familial cold autoinflammatory syndrome by interleukin-1 receptor antagonist. Lancet 2004;364:1779–85.
43. Hoffman HM, Throne ML, Amar NJ, et al. Efficacy and safety of rilonacept (interleukin-1 Trap) in patients with cryopyrin-associated periodic syndromes: results from two sequential placebo-controlled studies. Arthritis Rheum 2008;58:2443–52.
44. Lachmann HJ, Kone-Paut I, Kuemmerle-Deschner JB, et al, Canakinumab in CAPS Study Group. Use of canakinumab in the cryopyrin-associated periodic syndrome. N Engl J Med 2009;360:2416–25.
45. Lich JD, Ting JP. Monarch-1/pypaf7 and other CATERPILLER (CLR, NOD, NLR) proteins with negative regulatory functions. Microbes Infect 2007;9:672–6.
46. Gandhi C, Healy C, Wanderer AA, et al. Familial atypical cold urticaria: description of a new hereditary disease. J Allergy Clin Immunol 2009;124:1245–50.
47. Bonnetblanc JM, Andrieu-Pfahl F, Meraud JP, et al. Familial aquagenic urticaria. Dermatologica 1979;158:468–70.
48. Michaelsson G, Ros AM. Familial localized heat urticaria of delayed type. Acta Derm Venereol 1971;51:279–83.
49. Epstein PA, Kidd KK. Dermo-distortive urticaria: an autosomal dominant dermatologic disorder. Am J Med Genet 1981;9:307–15.
50. Jedele KB, Michels VV. Familial dermographism. Am J Med Genet 1991;39:201–3.

Japanese Clinical Medicine

REVIEW

Hereditary Disorders with Defective Repair of UV-Induced DNA Damage

Shinichi Moriwaki

Department of Dermatology, Osaka Medical College, Takatsuki, Japan.
Corresponding author email: der002@poh.osaka-med.ac.jp

Abstract: Nucleotide excision repair (NER) is an essential system for correcting ultraviolet (UV)—induced DNA damage. Lesions remaining in DNA due to reduced capacity of NER may result in cellular death, premature aging, mutagenesis and carcinogenesis of the skin. So, NER is an important protection against these changes. There are three representative genodermatoses resulting from genetic defects in NER: xeroderma pigmentosum (XP), Cockayne syndrome (CS), and trichothiodystrophy (TTD). In Japan, CS is similarly rare but XP is more common and TTD is less common compared to Western countries.
In 1998, we established the system for the diagnosis of these disorders and we have been performing DNA repair and genetic analysis for more than 400 samples since then. At present, there is no cure for any human genetic disorder. Early diagnosis and symptomatic treatment of neurological, ocular and dermatological abnormalities should contribute to prolonging life and elevating QOL in patients.

Keywords: UV-induced DNA damage, nucleotide excision repair, genodermatosis, DNA repair, skin cancer

Japanese Clinical Medicine 2013:4 29–35

doi: 10.4137/JCM.S10730

This article is available from http://www.la-press.com.

Introduction

Deoxyribonucleic acid (DNA), the basic substance of life, changes over the long term in the process of evolution, but strict homeostasis of DNA is important over the short term for the "maintenance of individual organisms."

DNA damage is thought to occur at the rate of tens of thousands events daily in each cell (endogenous DNA damage) while it is carrying out basic activities (normal metabolic processes) due to replication errors and oxidative damage. Exogenous factors (ultraviolet [UV] light, ionizing radiation, and environmental mutagens created by humans [tobacco smoke, exhaust fumes, etc.]) also cause DNA damage, so it is constantly occurring within living organisms. If the damage affects an important part of the genome, mutation, replication arrest, or inhibition of transcription may occur, leading to impairment of cellular function, cell death, aging, carcinogenesis, or even death of the organism. However, organisms are not defenseless against DNA damage, because various "DNA repair systems" have been developed in the course of evolution to efficiently repair "harmful" DNA damage via very precise mechanisms that involve many proteins functioning in an integrated fashion.

Xeroderma pigmentosum (XP) is a "human" mutation that causes hypersensitivity to UV radiation, resulting in inherited severe photosensitivity, which was initially described by the Austrian dermatologist Kaposi at the end of the 19th century.[1,2] The first breakthrough in the study of XP, however, was only achieved when the radiation biologist Cleaver found that it was caused by abnormal removal/repair of UV-induced DNA damage.[3] Like XP, Cockayne syndrome (CS) and trichothiodystrophy (TTD) are also diseases caused by a human mutation leading to defective DNA repair.

UV-Induced DNA Damage

Human DNA consists of 3 billion base pairs. It is constantly exposed to exogenous factors that cause damage (UV light, ionizing radiation, environmental mutagens, drugs, etc.), coupled with endogenous factors such as metabolites, reactive oxygen species, and replication errors, resulting in new DNA damage at every moment. DNA damage can be classified into the following 8 types based on the structural changes that occur (Fig. 1). Among these, type 1 is caused by solar

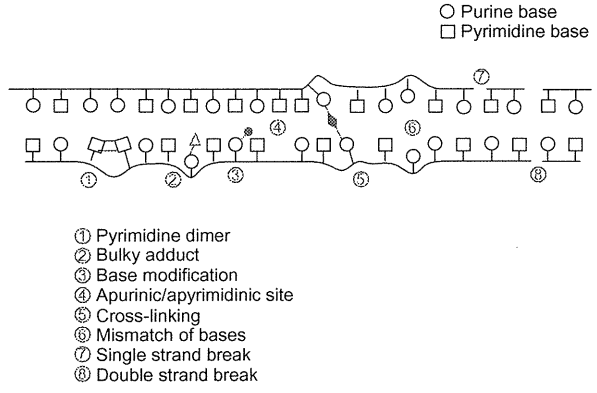

Figure 1. Spontaneous and environmental damage to DNA.

UV radiation (UVC, UVB and UVA2) (not visible light) that leads to dimerization of two adjacent pyrimidine bases. There are two known types of pyrimidine bases (Fig. 2). Successive pyrimidine bases can be activated by UV radiation, resulting in dimerization via a covalent bond between the C5 and C6 positions to create a cyclobutane pyrimidine dimer (CPD). Alternatively, a bond between the C6 position on the 5′ side and the C4 position on the 3′ side causes distortion, generating a (6-4) pyrimidine pyrimidone dimer photoproduct (6-4PP). Of all DNA damage caused by UV irradiation, the former type accounts for 75% and the latter for 25%. Repair of CPD is a relatively slow process, and damage still persists at 24 hours after UV irradiation. On the other hand, repair of 6-4PP is rapid and the damage is almost completely eliminated after 3 hours. Furthermore, lethality is frequent with the former type of mutation, whereas the latter is associated with a high rate of mutagenicity. In Figure 1, ③ is called base modification, and this change does

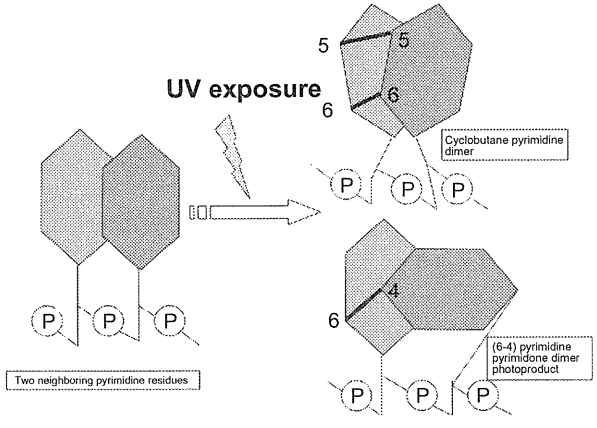

Figure 2. Two major alterations in DNA induced by UV.

not cause distortion of DNA. Oxidation of a guanine base to 8-oxo-guanine is a typical example.

DNA Repair of UV-Induced DNA Damage

Living organisms have DNA repair systems in order to maintain the integrity of DNA that carries the genetic code for life. These repair systems can cope with various types of DNA damage and are divided into 6 categories, including photoreactivation, dealkylation of alkylated bases, direct repair of damage (eg, repair of single-strand or double-strand breaks), excision repair, recombination repair, or post-replication repair (translesion DNA synthesis).

Photoreactivation utilizes long-wavelength UV light and visible light to repair pyrimidine dimers produced by exposure to UV radiation. Depending on the type of DNA damage, a covalent bond of a dimer is cut by electron transfer through the activity of two enzymes (CPD photolyase and 6-4 photolyase). However, this system does not exist in placental mammals such as humans.

The excision repair system includes a base excision repair (BER) mechanism and a nucleotide excision repair (NER) mechanism. Most oxidative DNA damage is repaired by the former mechanism. Recently, an association between the onset of neurological symptoms of XP and abnormalities of this repair mechanism has been pointed out.[4] The latter is the most important DNA repair mechanism (Fig. 3), and it plays a role in the removal of CPDs and 6-4PPs. This repair mechanism can remove relatively large DNA regions encompassing dozens of bases as a complete unit, and is the mechanism most frequently involved in the pathogenesis of XP, CS and TTD. In NER, there are two main pathways, global genome repair (GGR) and transcription-coupled repair (TCR) and each pathway includes 4 steps; these are damage recognition, DNA unwinding, incision/DNA excision and de novo synthesis.[5] Post-replication repair (ie, translesion DNA synthesis) is a back-up repair system for the NER mechanism that acts slowly and attempts to bypass residual CPD sites. In XP variant (XPV), the NER mechanism functions properly, but there are defects of the post-replication repair system (Fig. 3).[6]

Xeroderma Pigmentosum (XP)

Xeroderma pigmentosum is a rare photosensitive dermatosis with autosomal recessive inheritance that is caused by abnormalities of the repair mechanisms for UV-induced DNA damage and is associated with a high frequency of skin cancer.[7,8] The frequency of XP in Japan is 1 person in tens of thousands, but this

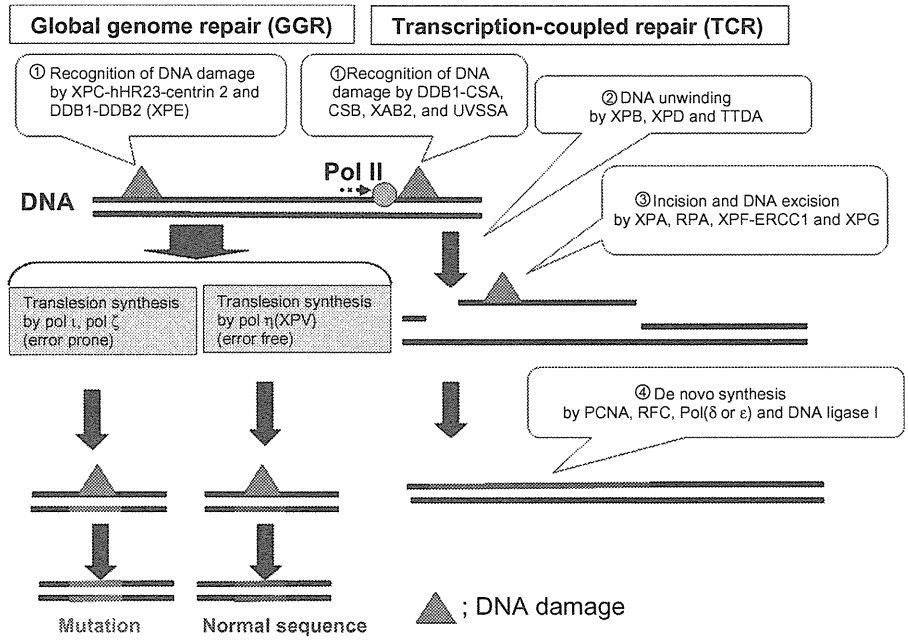

Figure 3. The pathway of nucleotide excision repair and translesion synthesis.

prevalence is more than 10 times higher compared with that in Europe and the United States.[9]

In a typical case, the skin of the face and other sun-exposed areas is affected by repeated severe sunburn from early childhood (Fig. 4A), resulting in abnormal freckle-like pigmentation (Fig. 4B). A phototest will reveal a marked decrease of the minimal erythema dose and a severe delayed erythema reaction. Should patients fail to carry out strict sun protection, skin tumors such as basal cell carcinoma, solar keratosis, squamous cell carcinoma and melanoma will occur frequently from an early age, with the risk being more than 1,000 times higher than in healthy individuals. Progressive central and peripheral neurological degeneration are observed in 30% of all XP patients (60% of Japanese patients), but the underlying mechanisms remain unknown. There are several genetically distinct types of XP that are categorized into a total of eight groups. These include seven groups (A to G) with NER abnormalities and one variant that has normal NER function but defective post-replication repair. The progression of symptoms, severity, and prognosis are different for each group.[9] The groups that present with characteristic neurological symptoms of XP are XPA, XPD, and XPG. In XPB, all patients have CS (see below), whereas some XPD patients have both CS and TTD (see below). Some XPG patients also have CS. In Japan, XPA patients with severe dermatological and neurological symptoms accounts for 54%, followed by the XP variant with only dermatological symptoms, accounting for 25%. On the other hand, XPC patients without neurological symptoms are common (40%) in Europe and the United States. Almost all XPA patients develop central or peripheral neurological complications, including impaired psychomotor development, and the severity of their neurological defects influences the prognosis. Based on the clinical diversity of XP, it can be classified as "the cutaneous type" with skin symptoms only, "the neurological type" with XP neurological symptoms, "the CS type" with symptoms of CS, and "the TTD type" with symptoms of TTD.[10] However, the association between clinical features/biological characteristics of XP (decrease of UDS and marked decrease of cell viability after UV irradiation) (phenotype) and the type or location of the *XP* gene mutation (genotype) has not been clarified.

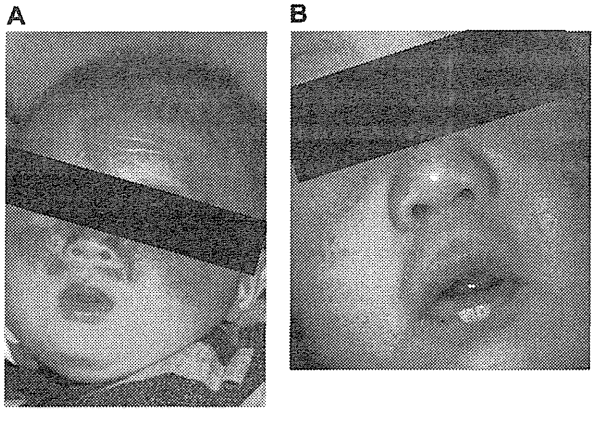

Figure 4. Clinical features of patients with xeroderma pigmentosum group A (XPA). (**A**) Severe sunburn (a newborn baby). (**B**) Abnormal pigmentation appears after repeated episodes of sunburn (a 3-month-old boy).

Cockayne Syndrome (CS)

CS was first reported in 1946 by the British pediatrician Cockayne as "a case with a marked decrease in growth accompanied by atrophy of the optic nerve and hearing loss".[11] Similar to XP, it is an extremely rare autosomal recessive disorder (1 in 0.5–1 million) that occurs due to failure of the NER mechanism, a major repair system for UV-induced DNA damage, especially for damage at sites of transcription. Over 200 cases have been reported in Europe and the United States, whereas there have been about 70 cases reported in Japan.

Symptoms of photosensitivity start to occur around six months after birth. Diverse features can be noted, such as microcephaly, a distinct facies (an aged look, sunken eyes, beak-like nose, big ears, protruding upper jaw), short stature, malnutrition, poor growth, pigmentary retinal degeneration, hearing loss, and mental retardation. These findings are not at all apparent immediately after birth, but start to appear around the age of 2 years and progress with aging. Freckle-like pigmentation of sun-exposed areas, as seen in patients with XP, and skin cancer are absent in patients with CS, except for those with XP/CS. Calcification of the brain is observed on head computed tomography (CT) and this finding is of high diagnostic value. Impaired liver and kidney function and diabetes mellitus occur as complications, and 80% of patients die before the age of 20 years due to infections such as pneumonia.[12] There are also rare mild cases where the onset is delayed.[12] Clinically, CS is classified into 3 types: a classic

type (type 1) in which patients survive until around the time of puberty, a severe type (type 2) in which patients die in infancy, and a delayed or adult-onset mild type (type 3). Types 2 and 3 are very rare.

2 genetically different types exist (groups A and B), with 25% being CSA and 75% being CSB. The defective proteins CSA (also called ERCC8; the gene responsible is at chromosome 10q11.23) and CSB (ERCC6; the gene responsible is at chromosome 5q12.1) are essential for the NER mechanism and both act in the early phase of TCR.

Diseases that exhibit the CS phenotype can be classified into 5 types according to the genes responsible, which are (1) CSA, (2) CSB, (3) CS/XPB, (4) CS/XPD, and (5) CS/XPG. Among these, types 3, 4, and 5 are referred to as "XP/CS complex", with each type being attributed to mutation of the *XPB* gene, *XPD* gene, and *XPG* gene, respectively. In types 1 and 2, patient cells maintain normal GGR, but TCR defects lead to impaired cell viability and a markedly decreased ability to synthesize ribonucleic acid (RNA) after UV irradiation, despite normal unscheduled DNA synthesis (UDS), which is an indicator of GGR. Types 3, 4, and 5 are complicated by XP, and occur due to mutations of the *XPB*, *XPD*, and *XPG* genes, respectively, with the clinical picture sometimes including abnormal facial pigmentation and malignant skin tumors in addition to features of CS. Because many of the factors associated with the NER system involved in the pathogenesis of CS also affect transcription, these patients can have various symptoms in addition to symptoms related to premature aging.

Cerebro-oculo-facio-skeletal (COFS) syndrome is a disorder with the main characteristics of congenital microcephaly, congenital cataract, microphthalmia, progressive arthrogryposis, and severe growth failure. Recently, a genetic mutation of *CSB* has been found, that is considered to represent a subtype of CS, and its relation to the *XPD* or *ERCC1* genes has been suggested in some reports.[13–15]

Trichothiodystrophy (TTD)

TTD is known as sulfur-deficient brittle hair syndrome, since the main symptoms of this extremely rare autosomal recessive congenital disease include hair abnormalities due to a decreased sulfur content, accompanied by various other symptoms such as short stature, ichthyosis, mental retardation, abnormal nail plates, abnormal teeth, and infertility. Photosensitivity is also observed in 40% of these patients. The characteristic of this disease is short and brittle hair (trichorrhexis nodosa or trichoschisis) due to a low content of cysteine, one of the sulfur-containing amino acids. Observation under a polarizing microscope reveals a yellow and black striped pattern known as tiger tail banding. According to statistics from the United States, TTD patients also have mental retardation (86%), short stature (73%), and ichthyosis (65%).[16,17] Genetically, there are three types of the photosensitive form of TTD: (1) the TTDA type with no functional GGR or TCR, high sensitivity to UV radiation, and low UDS; (2) a type with *XPG* gene mutation; and (3) a type with *XPD* gene mutation. Of these, the third type is the most common (85%), while the first and second types are very rare. The protein responsible for TTDA is a component of TFIIH, which has recently been revealed to be TFB5 (GTF2H5) involved in both transcription and NER.[18] Because TTDA, XPB, and XPD are all components of TFIIH, it is speculated that symptoms of TTD other than hypersensitivity to sunlight may be due to abnormalities of transcription. On the other hand, in the non-photosensitive form of TTD, the responsible gene is TTDN1 (C7orf11), which is only involved in transcription and is not a component of TFIIH. The frequency has been reported to be 1 in 1 million persons for Europe and the United States, while only 2 cases have been reported in Japan (unconfirmed group and TTD-A in 1 case each).

Diagnosis of XP, CS, and TTD

Definitive diagnosis of the above-mentioned diseases is mainly achieved by using cultured fibroblasts from the patient's skin to perform the following tests: (1) measurement of UDS after UV irradiation, (2) assessment of UV light sensitivity (with or without caffeine), (3) assessment of the level of DNA repair and a complementation test, and (4) genetic or protein analysis. In patients with XP (excluding XPV) and TTD, cells are hypersensitive to killing by UV, and UDS is reduced to less than 50% of that in normal cells. Cells from CSA and CSB patients are highly sensitive to UV radiation and show normal levels of UDS/impaired synthesis of RNA after UV irradiation. The possibility of XPV becomes higher if caffeine increases UV sensitivity. XPA accounts for the

majority of XP in Japan, and a homozygous mutation (G to C) at the 3′ splice acceptor site of intron 3 of the *XPA* gene is detected in 79% of patients, while a heterozygous mutation is detected in 16%. In addition, there is a homozygous mutation involving exon 6 (R228X) in 2% and a heterozygous mutation in 9%. These abnormalities (IVS3-1G > C, R228X) represent *XPA* gene mutation hot spots for Japanese patients (the former is the major hot spot and the latter is the minor hot spot), and both mutations can be easily identified by PCR-restriction fragment length polymorphism analysis (*AlwN I, Hph I*).[9,19] Due to the strong founder effect, accurate genetic testing can be performed rapidly in most Japanese patients with XPA, and this is also utilized in genetic services such as carrier detection[20] and prenatal diagnosis. Definitive diagnosis of other XP groups, CS and TTD can be achieved by a genetic complementation test that assesses the ability of patient cells to reactivate a reporter gene (eg, a luciferase expression vector) after UV damage. It is difficult, however, to obtain a definitive diagnosis of XPE and XPV with this complementation test, so protein and genetic analyses are required.[22]

Figure 5. Sun protective hood used in a case of XPA.

Patient Management (eg, Protection Against Ultraviolet Radiation)

Since XP, CS, and TTD are all genetic disorders, a cure cannot be expected. Therefore, strict and complete lifetime protection from UV radiation for prevention of complications is the basic policy for patients with these diseases.

As measures for protection against sunlight, patients are instructed to use a topical sunscreen with a high SPF value and high PA grade, and are told to wear tops with long sleeves, long pants, a hat, UV protective clothing, and UV protective glasses when they go out. Achieving complete UV protection stops the progression of freckle-like pigmentation and suppresses the development of malignant skin tumors (Fig. 5).

As for the neurologic defects associated with XP and CS, there are no effective evidence-based treatment measures because the pathogenesis is still unclear. Intake of a diet rich in vitamin C, vitamin E, and catechin (which have an antioxidant effect) stimulation of the brain, and encouragement of movement from early childhood may prevent neurological symptoms from advancing. Older children should regularly attend a rehabilitation service for the purpose of delaying movement disorder and preventing contractures.

Due to the need for "lifelong protection from sunlight," patients with inherited photosensitivity diseases have an impaired quality of life (QOL). Because patients with XP, CS, and TTD also have various specific complications, QOL is further decreased for these patients and their families. In other words, patients and families suffer from severe physical, mental, and economic stress due to the heavy burdens of "strict lifetime UV protection," "complications, children with disabilities," "incurable disease," and "genetic problems". Adequate care for patients with such diseases and support for their families cannot be provided by physicians alone. Under such circumstances, there is an important role for patient and family advocacy groups, which are founded with the objectives of sharing knowledge about diseases and ideas or information for daily living, sharing enjoyment, and making

society aware of these rare diseases in order to improve the healthcare environment. The activities of such patient and family advocacy groups are naturally patient/family-driven, but physicians and researchers involved with these diseases also offer positive support through provision of information and other assistance.

Acknowledgments

The present work was supported by Grants-in-Aid for Scientific Research (No. 24591639) and by "Research on Measures for Intractable Diseases" Project: matching fund subsidy from the Ministry of Health, Labour and Welfare.

Author Contributions

The author designed the present project, analyzed the data and wrote the manuscript. The author reviewed and approved the final version.

Funding

Author(s) disclose no funding sources.

Competing Interests

Author(s) disclose no potential conflicts of interest.

Disclosures and Ethics

As a requirement of publication author(s) have provided to the publisher signed confirmation of compliance with legal and ethical obligations including but not limited to the following: authorship and contributorship, conflicts of interest, privacy and confidentiality and (where applicable) protection of human and animal research subjects. The authors have read and confirmed their agreement with the ICMJE authorship and conflict of interest criteria. The authors have also confirmed that this article is unique and not under consideration or published in any other publication, and that they have permission from rights holders to reproduce any copyrighted material. Any disclosures are made in this section. The external blind peer reviewers report no conflicts of interest.

References

1. Hebra F, Fagge CH, Kaposi M. *On Diseases of the Skin, Including the Exanthemata, Volume* 3. London: New Sydenham Society; 1874.
2. Kaposi M. Xeroderma pigmentosum. *Ann Dermatol Venereol.* 1883;4: 29–38.
3. Cleaver JE. Defective repair replication of DNA in xeroderma pigmentosum. *Nature.* 1968;218:652–6.
4. Hayashi M. Role of oxidative stress in xeroderma pigmentosum. *Adv Exp Med Biol.* 2008;637:120–7.
5. Kraemer KH, Patronas NJ, Schiffmann R, Brooks BP, Tamura D, DiGiovanna JJ. Xeroderma pigmentosum, trichothiodystrophy and Cockayne syndrome: a complex genotype-phenotype relationship. *Neuroscience.* 2007;145:1388–96.
6. Cordonnier AM, Fuchs RP. Replication of damaged DNA: molecular defect in xeroderma pigmentosum variant cells. *Mutat Res.* 1999;435:111–9.
7. Kraemer KH, Lee MM, Scotto J. Xeroderma pigmentosum. Cutaneous, ocular, and neurologic abnormalities in 830 published cases. *Arch Dermatol.* 1987;123:241–50.
8. Bradford PT, Goldstein AM, Tamura D, et al. Cancer and neurologic degeneration in xeroderma pigmentosum: long term follow-up characterises the role of DNA repair. *J Med Genet.* 2011;48:168–76.
9. Moriwaki S, Kraemer KH. Xeroderma pigmentosum—bridging a gap between clinic and laboratory. *Photoderm Photoimmun Photomed.* 2001;17:47–54.
10. Rapin I, Lindenbaum Y, Dickson DW, Kraemer KH, Robbins JH. Cockayne syndrome and xeroderma pigmentosum. *Neurology.* 2000;55:1442–9.
11. Cockayne EA. Dwarfism with retinal atrophy and deafness. *Arch Dis Child.* 1946;21:52–4.
12. Nance MA, Berry SA. Cockayne syndrome: Review of 140 cases. *Am J Med Genet.* 1992;42:68–84.
13. Meira LB, Graham JM Jr, Greenberg CR, et al. Manitoba aboriginal kindred with original cerebro-oculo-facio-skeletal syndrome has a mutation in the Cockayne syndrome group B (CSB) gene. *Am J Hum Genet.* 2000;66: 1221–8.
14. Graham JM Jr, Anyane-Yeboa K, Raams A, et al. Cerebro-oculo-facio-skeletal syndrome with a nucleotide excision-repair defect and a mutated XPD gene, with prenatal diagnosis in a triplet pregnancy. *Am J Hum Genet.* 2001;69:291–300.
15. Jaspers NG, Raams A, Silengo MC, et al. First reported patient with human ERCC1 deficiency has cerebro-oculo-favio-skeletal syndrome with a mild defect in nucleotide excision repair and severe developmental failure. *Am J Hum Genet.* 2007;80:457–66.
16. Liang C, Morris A, Schlucker S, et al. Structural and molecular hair abnormalities in trichothiodystrophy. *J Invest Dermatol.* 2006;126:2210–6.
17. Faghri S, Tamura D, Kraemer KH, Digiovanna JJ. Trichothiodystrophy: a systematic review of 112 published cases characterises a wide spectrum of clinical manifestations. *J Med Genet.* 2008;45:609–21.
18. Giglia-Mari G, Coin F, Ranish JA, et al. A new, tenth subunit of TFIIH is responsible for the DNA repair syndrome trichothiodystrophy group A. *Nat Genet.* 2004;36:714–9.
19. Nishigori C, Moriwaki S, Takebe H, Tanaka T, Imamura S. Gene alterations and clinical characteristics of xeroderma pigmentosum group A patients in Japan. *Arch Dermatol.* 1994;130:191–7.
20. Hirai Y, Kodama Y, Moriwaki S, et al. Heterozygous individuals bearing a founder mutation in the XPA DNA repair gene comprise nearly 1% of the Japanese population. *Mutat Res.* 2006;601:171–8.
21. Moriwaki S, Yamashita Y, Nakamura S, et al. Prenatal diagnosis of xeroderma pigmentosum group A in Japan. *J Dermatol.* 2012;39:516–9.
22. Tanioka M, Masaki T, Ono R, et al. Molecular analysis of DNA polymerase eta gene in Japanese patients diagnosed as xeroderma pigmentosum variant type. *J Invest Dermatol.* 2007;127:1745–51.

ORIGINAL ARTICLE

Interaction of the Profilaggrin *N*-Terminal Domain with Loricrin in Human Cultured Keratinocytes and Epidermis

Kozo Yoneda[1], Toshitaka Nakagawa[2], Owen T. Lawrence[3], Jessica Huard[3], Toshio Demitsu[4], Yasuo Kubota[1] and Richard B. Presland[3,5]

The relationship between the two coexpressed differentiation markers, profilaggrin and loricrin, is not clear right now. In this study, we explored the interaction of profilaggrin *N*-terminal domain (PND) with loricrin in keratinocytes and epidermis. Confocal immunofluorescence microscopic analysis of human epidermis showed that PND colocalized with loricrin. Loricrin nucleofected into HaCaT cells colocalized with PND in the nucleus and cytoplasm. The PND localizes to both the nucleus and cytoplasm of epidermal granular layer cells. Nucleofected PND also colocalized with keratin 10 (K10) in the nucleus and cytoplasm. Immunoelectron microscopic analysis of human epidermis confirmed the findings in nucleofected keratinocytes. Yeast two-hybrid assays showed that the B domain of human and mouse PND interacted with loricrin. The glutathione *S*-transferase (GST) pull-down analysis using recombinant GST-PND revealed that PND interacted with loricrin and K10. Knockdown of PND in an organotypic skin culture model caused loss of filaggrin expression and a reduction in both the size and number of keratohyalin granules, as well as markedly reduced expression of loricrin. Considering that expression of PND is closely linked to keratinocyte terminal differentiation, we conclude that PND interacts with loricrin and K10 *in vivo* and that these interactions are likely to be relevant for cornified envelope assembly and subsequent epidermal barrier formation.

Journal of Investigative Dermatology (2012) **132,** 1206–1214; doi:10.1038/jid.2011.460; published online 26 January 2012

INTRODUCTION

The outermost layers of stratified squamous epithelia are composed of mechanically tough dead cornified cells (corneocytes), which are formed as a result of a complex terminal differentiation program (Yoneda *et al.*, 1992b; Kalinin *et al.*, 2001, 2002; Candi *et al.*, 2005). Cornified cells are devoid of all organelles and are encapsulated within a highly specialized structure termed the cornified envelope (CE). CE insolubility is due to disulfide bonding and cross-linking by N^{ε}-(γ-glutamyl)lysine isopeptide bonds formed by transglutaminases (EC2.3.2.13) (Steinert and Marekov, 1995, 1997; Yoneda *et al.*, 1998).

Upon terminal differentiation of granular cells, profilaggrin is proteolytically cleaved into ~37-kDa filaggrin peptides and ~32-kDa profilaggrin *N*-terminal domain (PND) containing the S100-like calcium-binding domain (Presland *et al.*, 1995; Dale *et al.*, 1997; Kuechle *et al.*, 1999; Pearton *et al.*, 2001, 2002; Sandilands *et al.*, 2009). The human PND comprises two distinct domains: an acidic A domain of 81 amino acids that binds Ca^{2+} and a cationic B domain of 212 residues (Presland *et al.*, 1992, 1997). The A domain contains two calcium-binding motifs that are similar to the EF-hands of the S100 family of calcium-binding proteins and is able to bind calcium *in vitro* (Presland *et al.*, 1995). The B domain is 212 amino acids in length, contains a high proportion of polar amino acids, and is predicted to have a cationic net charge. We previously raised five peptide antibodies directed to human and mouse A and B domains (A1, A2, B1, B2, and Am1 antibodies; Presland *et al.*, 1997; Pearton *et al.*, 2002). Using these antibodies we demonstrated that the PND was cleaved from the filaggrin sequences during epidermal differentiation and localized to the nucleus of dying transition cells, which suggested that PND might have an independent fate and/or function from filaggrin (Ishida-Yamamoto *et al.*, 1998).

[1]*Department of Dermatology, Faculty of Medicine, Kagawa University, Kagawa, Japan;* [2]*Department of Life Science Research Center, Faculty of Medicine, Kagawa University, Kagawa, Japan;* [3]*Department of Oral Health Sciences, University of Washington, Seattle, Washington, USA;* [4]*Department of Dermatology, Jichi Medical University, Saitama Medical Center, Saitama, Japan and* [5]*Division of Dermatology, Department of Medicine, University of Washington, Seattle, Washington, USA*

Correspondence: Kozo Yoneda, Department of Dermatology, Faculty of Medicine, Kagawa University, 1750-1 Ikenobe, Kagawa 761-0793, Japan. E-mail: kyoneda@med.kagawa-u.ac.jp

Abbreviations: 3-AT, 3-amino 1,2,4-triazole; cDNA, complementary DNA; CE, cornified envelope; DAPI, 4,6-diamidino-2-phenylindole; GST, glutathione S-transferase; K10, keratin 10; Lor, loricrin; PND, profilaggrin N-terminal domain; siRNA, small interfering RNA; SPRR, small proline-rich protein; Y2H, yeast two-hybrid

Received 15 June 2011; revised 23 October 2011; accepted 2 November 2011; published online 26 January 2012

Loricrin (Latin: "lorica"—a protective shell or cover) functions as a key structural CE protein (Mehrel *et al.*, 1990; Hohl *et al.*, 1991; Yoneda *et al.*, 1992a, 1992b, 2010b; Yoneda and Steinert, 1993). Loricrin is expressed in the granular layer during cornification, and is unusually rich in glycine, serine, and cysteine residues (Ishida-Yamamoto *et al.*, 1993, 1998). Loricrin is the chief component of the epidermal CE comprising 70–85% of the total protein mass of the CE.

In this paper, we report the colocalization of PND with loricrin and keratin 10 (K10) in human epidermis and HaCaT keratinocytes. We show that human PND interacts with both loricrin and K10 using yeast two-hybrid (Y2H) assays and immunoprecipitation of keratinocyte extracts. These studies demonstrate the presence of a network of interactions between CE and cytoskeletal proteins that are likely important for building the CE and the resulting epidermal permeability barrier.

RESULTS

The PND colocalizes with loricrin and K10 in epidermis and HaCaT keratinocytes

Antibodies generated against the A and B PND domains immunostained the cytoplasm of granular cells and the lower cornified layers (Figure 1a and Supplementary Figure S1a online). Filaggrin mAb AKH1 showed the typical particulate pattern staining throughout the granular cells with some staining of the stratum corneum (Figure 1a and Supplementary Figure S1a online).

To examine expression and colocalization of epitope-tagged PND and loricrin peptides in cultured keratinocytes, the PND construct pFLAG-467proF (Presland *et al.*, 1997) and loricrin-V5-His complementary DNAs (cDNAs) were nucleofected into HaCaT cells. At 48 hours after nucleofection, HaCaT cells grown on glass coverslips were fixed with methanol and immunolabeled with anti-V5 (to detect loricrin peptide) or A2 or B1 profilaggrin antibodies (Figure 1b and

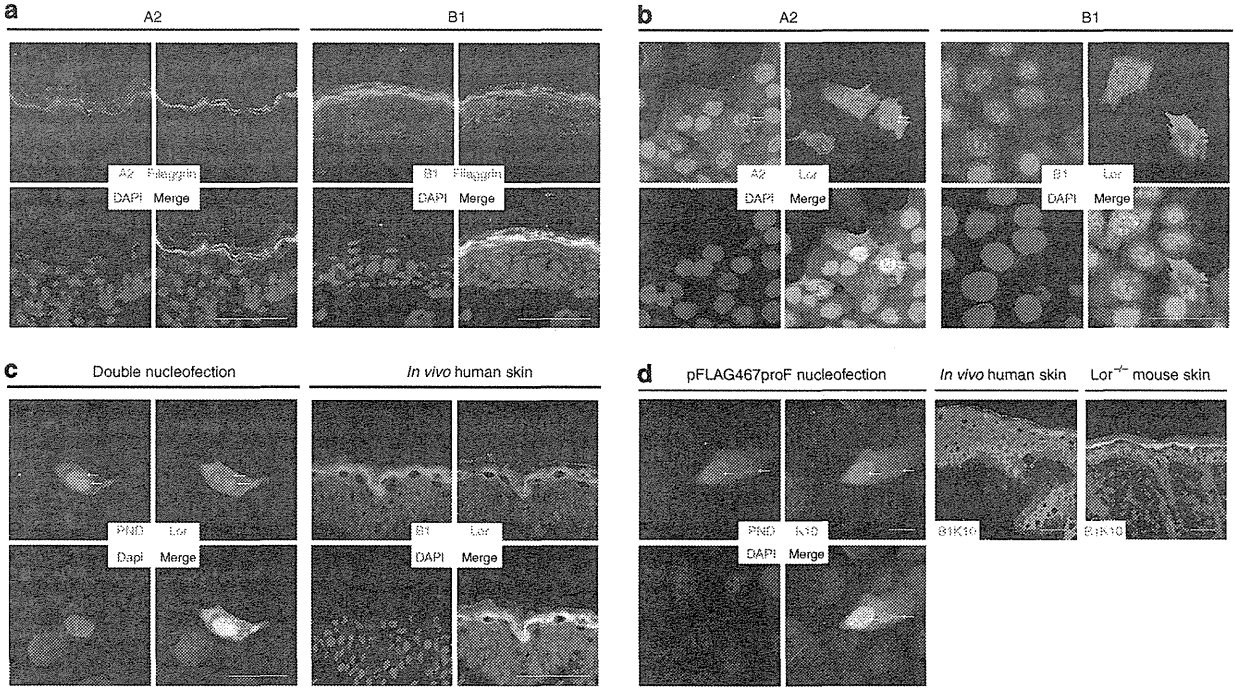

Figure 1. Expression of the A and B domains of profilaggrin N-terminal domain (PND) in human adult epidermis and HaCaT cells and colocalization with loricrin. (**a**) We prepared cryosections from optimal cutting temperature (OCT) compound-embedded normal human skin. We conducted double immunostaining with filaggrin mAb AKH1 and A2 or B1 antibody. A2 and B1 immunostained cytoplasm of granular layers and also showed some reaction with the lower stratum corneum. DAPI, 4,6-diamidino-2-phenylindole. Bars = 80 μm. (**b**) Distribution of PND in HaCaT cells nucleofected by pcDNA3.1/V5-His-loricrin. Nucleofected HaCaT cells were fixed at 48 hours after transfection, and the cells were stained with anti-V5 antibody and either A2 or B1 antibody. Nucleofected loricrin distributed diffusely in the cytoplasm and in the nuclei. PND also distributed in the nuclei abundantly and the cytoplasm in HaCaT cells. A substantial portion of nucleofected loricrin colocalized with PND (arrows). Bars = 50 μm. Interaction of PND and loricrin (Lor). (**c**) We doubly nucleofected pFLAG467proF and pcDNA3.1/V5-His-loricrin into HaCaT cells. Cells were fixed at 48 hours after transfection, and the fate of the transfected gene product was examined by double-label immunofluorescence. To visualize the nucleofected gene product, cells were doubly stained with a rabbit polyclonal antibody recognizing the sequence of FLAG tag and a mouse mAb recognizing the sequence of V5 tag. PND distributed in the nuclei and diffusely in the cytoplasm in nucleofected cells. PND and loricrin (Lor) colocalized not only in the cytoplasm but also in the nucleus (arrows). Bar = 25 μm. We also doubly stained *in vivo* human skin with B1 antibody and guinea pig polyclonal anti-loricrin antibody. PND and Lor colocalized in the cytoplasm of granular cells and the lower cornified cells. Bars = 80 μm. (**d**) We doubly stained HaCaT cells nucleofected with pFALG467proF with B1 antibody and mouse anti-K10 mAb. PND and keratin 10 (K10) colocalized not only in the nucleus but also in the cytoplasm. Bar = 10 μm. We doubly stained *in vivo* human skin with B1 antibody and mouse anti-K10 mAb. PND and K10 colocalized at granular layer and lower stratum corneum. We doubly stained $Lor^{-/-}$ mouse skin with B1 antibody and mouse anti-K10 mAb. PND and K10 colocalized at granular layer and lower stratum corneum. Bars = 80 μm.

Supplementary Figure S1b online), or with anti-FLAG and anti-V5 antibodies (Figure 1c and Supplementary Figure S1c online). The PND was found in the nucleus and cytoplasm of HaCaT cells, as previously reported in other cell culture systems (Pearton *et al.*, 2002). A substantial portion of transfected loricrin colocalized with endogenous PND protein in both the cytoplasmic and nuclear compartments of HaCaT cells (Figure 1b). Cells nucleofected with tagged PND and loricrin constructs confirmed the colocalization of PND and loricrin peptides in the cytoplasm and nucleus of HaCaT cells (Figure 1c and Supplementary Figure S1c online).

We next nucleofected pFLAG467proF into HaCaT cells and double-stained these nucleofected cells with anti-FLAG antibody and anti-K10 antibody. PND and K10 colocalized in both the cytoplasm and nucleus (Figure 1d). We double-stained human skin with B1 antibody and anti-K10 mAb. The PND and K10 colocalized in the cytoplasm of granular cells and the lower cornified layers. We also double-stained $Lor^{-/-}$ mouse skin with profilaggrin B1 antibody and anti-K10 mAb. In the absence of loricrin, the PND and K10 colocalized in the cytoplasm of granular cells and lower cornified layers (Figure 1d).

In order to more precisely define the interaction between PND and loricrin or between PND and K10, immunoelectron microscopy was performed using normal human epidermis. The A2 and B1 antibodies decorated keratohyalin granules in the granular layer and showed considerable labeling of the lower layers of stratum corneum. The PND and loricrin colocalized at the perimeter of large keratohyalin granules as well as within smaller, less electron-dense granules (Figure 2a). K10 and PND colocalized at the periphery of keratohyalin granules with K10 antibody labeling filaments juxtaposed to keratohyalin (Figure 2b). In $Lor^{-/-}$ mouse skin, K10 and PND also colocalized at the periphery of profilaggrin-containing F-granules (Figure 2c). Quantitative analysis also confirmed these results.

Biochemical evidence for association of the profilaggrin *N*-terminus with loricrin and K10

To identify proteins that interact with the PND, a mouse epidermal cDNA library was screened using the complete mouse profilaggrin *N*-terminus as bait. A total of 65 positive clones were initially obtained from the Y2H screen that was performed on histidine-deficient media containing 2.5 mM 3-AT (3-amino 1,2,4-triazole). A total of 15 distinct clones were positive by Y2H upon retesting after retransformation of purified plasmid DNAs into yeast. Among the interacting cDNAs/proteins were three CE or cytoskeletal proteins identified as loricrin, K10, and a SPRR (small proline-rich protein)-like protein that displays 95% identity to a SPRR10-like protein (Figure 3 and Table 1a). The PND interacts with the central glycine/serine-rich region of mouse loricrin, whereas it interacts with a fragment of K10 that includes most of the *C*-terminal tail domain and the distal portion of the α-helical rod domain (Table 1a). K10 and the SPRR-like protein interact strongly with the complete mouse profilaggrin *N*-terminus whereas loricrin interacts more weakly. However, loricrin associates strongly with the human and mouse B domain alone (Figure 3 and Table 1b). None of the yeast or human control proteins interacted with loricrin, K10, or the SPRR-like protein under medium- or high-stringency Y2H conditions. Notably, loricrin and the SPRR-like protein interact with the B domain alone, whereas K10 only bound to the complete mouse PND (Table 1b).

To confirm that loricrin associates with the PND, HaCaT cells were nucleofected with pcDNA3.1/V5-His-loricrin and pFLAG467proF. Nucleofected HaCaT cells were lysed in precipitation assay buffer and soluble lysates incubated with anti-FLAG antibody. Immunoblotting of precipitated proteins demonstrated the presence of both PND, loricrin and K10, indicating that PND associates with loricrin and K10 *in vitro* (Figure 4a). A direct association between PND and loricrin was probed *in vitro* by glutathione *S*-transferase (GST) pull-down analysis using recombinant GST-PND. Similarly a direct association between PND and K10 was probed *in vitro* by GST pull-down analyses using recombinant GST-PND. The results are indicative of specific protein–protein interactions (Figure 4b).

Effect of PND knockdown on organotypic raft cultures

To further investigate the molecular role of the PND, we conducted PND knockdown experiments in organotypic raft cultures. The raft culture keratinocyte system infected with pAxewit2-PNDsiRNA or pAxewit2 vector containing the scrambled sequence was analyzed. Immunohistochemistry revealed reduced expression of PND and filaggrin in raft culture keratinocyte system infected with pAxewit2-PNDsiRNA (Figure 5a). Reduced number and size of keratohyalin granules were observed in keratinocytes infected with pAxewit2-PNDsiRNA adenovirus as measured by electron microscopy (Figure 5b). Immunoblot analysis using B1 antibody revealed that the raft culture keratinocyte system infected with pAxewit2-PNDsiRNA did not express PND (Figure 5c). Immunoblot analysis using anti-K10 and anti-loricrin antibodies revealed that raft culture keratinocyte system infected with pAxewit2-PNDsiRNA expressed K10 and reduced amounts of loricrin, respectively (Figure 5c). We examined the expression of profilaggrin, K10, and loricrin mRNAs by real-time reverse-transcriptase–PCR. Profilaggrin mRNA was suppressed to 5.4% of the levels in cells infected with pAxewit2-PNDsiRNA. K10 mRNA was suppressed to 82.3% of the levels in infected cells. Loricrin mRNA was suppressed to 4.6% of the levels in infected cells (Figure 5d). The reason why loricrin mRNA was knocked down by the PND small interfering RNA (siRNA) is not clear right now. There may be off-target effect by their siRNA. Glycine and serine content of CE was reduced in infected cells (Supplementary Table S1 online).

DISCUSSION

It has previously been shown that the PND is cleaved from profilaggrin during epidermal terminal differentiation, where it localizes to both the nucleus and cytoplasm within granular, transition, and cornified cells (Presland *et al.*, 1997; Ishida-Yamamoto *et al.*, 1998; Pearton *et al.*, 2002). However, its potential role in keratinocyte differentiation and

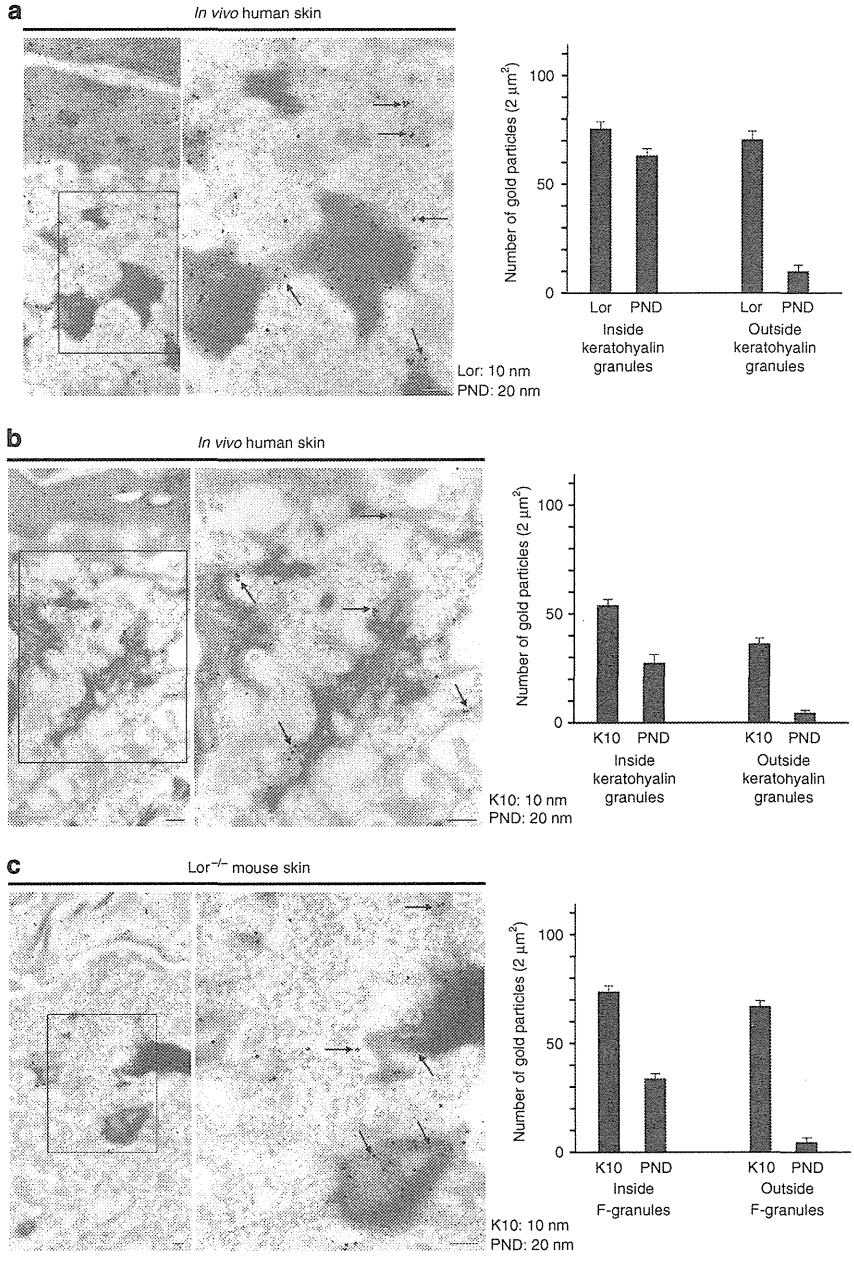

Figure 2. Profilaggrin *N*-terminal domain (PND) colocalized not only with loricrin (Lor) but also keratin 10 (K10). (**a**) Post-embedding immunoelectron microscopy using LR White resin method for *in vivo* human skin. B1 antibody and guinea pig polyclonal anti-loricrin antibody were used and labeled with 20 and 10 nm immunogold, respectively. PND signals were decorated in the keratohyalin granules. Loricrin (Lor) labels were closely associated with PND signals (arrows). (**b**) Post-embedding immunoelectron microscopy using LR White resin method for *in vivo* human skin. B1 antibody and mouse anti-K10 mAb were used and labeled with 20 and 10 nm immunogold, respectively. K10 labels were closely associated with PND signals (arrows). (**c**) Post-embedding immunoelectron microscopy using LR White resin method for $Lor^{-/-}$ mouse skin. B1 antibody and mouse anti-K10 mAb were used and labeled with 20 and 10 nm immunogold, respectively. K10 labels were closely associated with PND signals (arrows). Quantitative analysis also confirmed these results.

barrier formation is unknown. In this study we focused on the interaction between the PND and loricrin. Using the Y2H assay, immunoprecipitation experiment, and GST pull-down analysis, we demonstrated that loricrin associates with the PND, confirming immunofluorescence and immunoelectron microscopy findings showing colocalization in epidermis and transfected HaCaT cells. The PND also associates with K10, a protein that functions both as a CE protein and cytoskeletal intermediate filament protein (Kalinin *et al.*, 2001).

The importance of calcium in regulating epidermal differentiation *in vitro* has been recognized for many years (Elias *et al.*, 2002). Moreover, there is considerable evidence

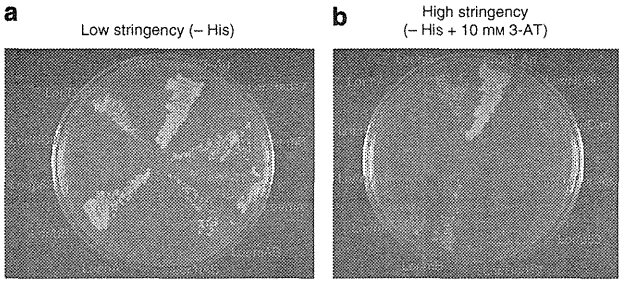

Figure 3. Loricrin (Lor) interacts with the profilaggrin *N*-terminus in yeast. Prey (AD-loricrin) and bait combinations were transformed into yeast and grown on either (**a**) histidine, leucine, and typtophan (HLT)-deficient plates or (**b**) HLT-deficient plates containing 10 mM 3-amino 1,2,4-triazole (3-AT). Fusion proteins consisting of GAL4 activation domain-loricrin interact with various mouse (m) or human (h) profilaggrin *N*-terminus peptide (AB or B domains alone), but not with human or mouse A domain alone, S100A2 (A2), human p53, or a series of yeast complementary DNAs (cDNAs; DAD, ND80, and RAD17) expressed as fusion protein with the GAL4 DNA-binding domain.

Table 1a. The mouse profilaggrin *N*-terminus interacts with cornified envelope-associated proteins and keratin 10 (K10)

Gene/ protein name	Genbank no.	Number of clones obtained	Region involved in interaction	Strength of interaction with mouse AB[2]
Loricrin (LOR)	NP_032534	1	109-388 (486)[1]	+
K10 (KRT10)	P02535	1	410-566 (570)[1]	+++
SPRR10-like	NP_079696	5	2-182 (182)[1]	+++

Abbreviation: SPRR, small proline-rich protein.
[1]Size of protein in amino acids.
[2]"+" Indicates growth in the absence of histidine plus 2.5 mM 3-amino 1,2,4-triazole (3-AT); "++" indicates growth in histidine-deficient media plus 10 mM 3-AT; "+++" indicates growth in histidine-deficient media plus 20 mM 3-AT.

Table 1b. Loricrin, K10, and the SPRR10-like protein interact with the B domain of mouse profilaggrin

Gene/ protein name	Interacts with mouse proFG AB[1]	Interacts with mouse proFG B	Interacts with mouse proFG A	Interacts with human proFG AB or B
Loricrin (LOR)	+	++	–	+++ (B)
K10 (KRT10)	+++		–	–
SPRR10-like	+++	+++	–	++ (AB)

Abbreviations: FG, filaggrin; K10, keratin 10; SPRR, small proline-rich protein.
[1]See Table 1 for description of yeast two-hybrid (Y2H) assay conditions.

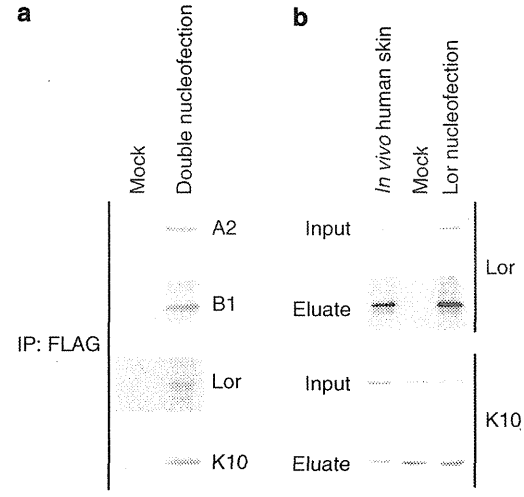

Figure 4. Association of the profilaggrin *N*-terminus with loricrin and keratin 10 (K10). (**a**) HaCaT cell were doubly nucleofected with pFLAG467proF and pcDNA3.1/V5-His-loricrin. The cells were lysed and processed for FLAG immunoprecipitation (IP) followed by A2, B1, loricrin (Lor), and K10 immunoblotting ($n=4$). The immunoprecipitates of FLAG contained loricrin and K10. (**b**) Glutathione *S*-transferase (GST) pull-down assays. GST-tagged profilaggrin *N*-terminal domain (PND) was immobilized on glutathione beads and probed for an interaction with Lor and K10. Binding of GST-tagged PND to loricrin or K10 was determined by immunoblot analyses ($n=4$).

for epidermal calcium gradient *in vivo*, which is abrogated by barrier disruption (Mauro *et al.*, 1998). Profilaggrin is processed by several calcium-regulated endoproteases to generate two major products, filaggrin and the PND. S100 proteins are a family of low-molecular-weight proteins characterized by two calcium-binding EF-hands (Deshpande *et al.*, 2000; Donato, 2001; Broome *et al.*, 2003; Eckert *et al.*, 2004). It is well known that S100 proteins serve as calcium sensors that, upon activation, regulate the subcellular distribution and/or function of specific target proteins. S100A2, a S100 family member, was shown to be expressed in the cytoplasm and nucleus of normal human keratinocytes and HaCaT cells (Deshpande *et al.*, 2000; Zhang *et al.*, 2002). This distribution pattern is very similar to the PND. Thus, the PND may act like an S100 protein in the keratinocyte, and loricrin appears to be one target protein of the PND; our results show that K10 is another target. Cultured keratinocytes generally show both nuclear and cytoplasmic staining of PND (Pearton *et al.*, 2002). While *in vivo*, staining of PND is mostly cytoplasmic (Presland *et al.*, 1997; Ishida-Yamamoto *et al.*, 1998). *In vivo*, the protein may be mostly in the form of profilaggrin, with the PND attached to the rest of the protein. Thus, immunolabeling is mostly cytoplasmic, especially at keratohyalin granules. Only in transition cell, or very occasionally in granular cells, nuclear labeling is seen (Ishida-Yamamoto *et al.*, 1998). This is presumably because the PND is removed from the rest of the protein, allowing it to localize to the nucleus. In HaCaT cells doubly nucleofected with pFLAG467proF and pcDNA3.1/V5-His-loricrin, the protein is not localized to keratohyalin granules but rather can distribute between the cytoplasm and nucleus. In addition, the lack of filaggrin domains in these short *N*-terminal

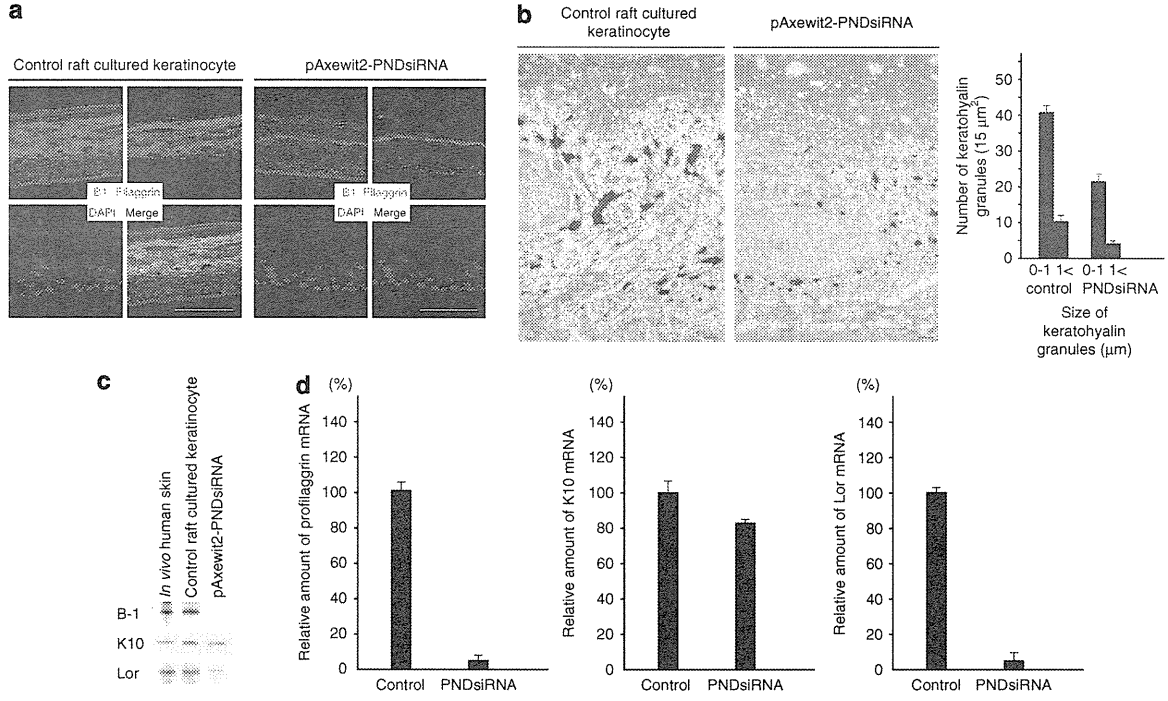

Figure 5. Expression of profilaggrin *N*-terminal domain (PND) is efficiently blocked by PND small interfering RNA (siRNA) in raft culture keratinocyte system. (**a**) In the raft culture keratinocyte system infected with pAxewit2-PNDsiRNA, immunostaining intensity of PND and filaggrin was reduced. DAPI, 4,6-diamidino-2-phenylindole. (**b**) Histogram quantitating the keratohyalin granules. For quantitation of keratohyalin granules, randomly selected cells were photographed and printed at a final magnification of 60,000. The numbers of keratohyalin granules in six different squares were counted. Sizes of keratohyalin granules were also graded. This electron microscopic analysis revealed that both number and size of keratohyalin granules were reduced in the raft culture keratinocyte system infected with pAxewit2-PNDsiRNA. (**c**) Immunoblot analysis using B1 antibody revealed that raft culture keratinocyte system infected with pAxewit2-PNDsiRNA did not express PND. Immunoblot analysis using anti-K10 and anti-loricrin antibodies revealed that raft culture keratinocytes infected with pAxewit2-PNDsiRNA expressed keratin 10 (K10) and reduced the amount of loricrin (Lor), respectively ($n=4$). (**d**) Real-time reverse-transcriptase-PCR (RT-PCR) analysis of the expression of profilaggrin, K10, and Lor mRNAs. Profilaggrin mRNA was suppressed to 5.4% of the levels in cells infected with pAxewit2-PNDsiRNA. K10 mRNA was suppressed to 82.3% of the levels in infected cells. Lor mRNA was suppressed to 4.6% of the levels in infected cells.

peptides means that the protein is not bound to keratin filaments, and thus not restricted to the cytoplasm. Although loricrin is also observed in the nucleus in doubly nucleofected HaCaT cells, this may be because of the fact that overexpressed loricrin exists in nucleus (Yoneda *et al.*, 2010a, 2010b). In HaCaT cells singly nucleofected with pFLAG467proF, K10 is localized in nucleus. Initiation of keratin filament assembly occurs at discrete sites on the nuclear envelope and filaments grow from the nucleus toward the cytoplasm (Albers and Fuchs, 1989). K10 molecules just before filament assembly may be transported into the nucleus via PND in pFLAG467proF-transfected HaCaT cells. The PND colocalized with K10 in both normal human epidermis and Lor$^{-/-}$ mouse skin. Both loricrin and the B domain of PND have a very similar amino-acid composition, consisting of quasi-repetitive, glycine-rich peptide sequences termed glycine loops, which might facilitate their protein–protein interaction (Backendorf and Hohl, 1992).

Previously, it was proposed that S100 proteins produced in keratinocytes could act as "envelope organizer proteins," acting to shuttle CE precursors to the site of CE assembly where transglutaminases crosslink the CE precursors (Robinson *et al.*, 1997; Eckert *et al.*, 2004). Several S100 proteins including S100A7, A10, and A11 have been shown to be transglutaminase substrates (Ruse *et al.*, 2001). The PND may be acting in a similar manner, acting to transport loricrin, K10, and other proteins to the site of CE assembly. Its Ca^{2+}-binding ability may help to promote the CE crosslinking and assembly process (Presland *et al.*, 1995). Immunoelectron microscopy data with a profilaggrin A domain antibody showing immunolabeling of CEs within the stratum corneum suggested that at least part of the PND is incorporated into CEs (Presland *et al.*, 1997). Recently, Okada *et al.* (2004) found that S100A1 also had chaperone ability. They demonstrated that thermal aggregation of citrate synthase, aldolase, glyceraldehyde-3-phosphate dehydrogenase, and rhodanase was inhibited by S100A1. S100A1 suppressed aggregation of denatured substrate during the refolding pathway. The chaperones can interact with various cytoplasmic proteins nonspecifically, which contrasts with PND that has a limited number of cytoplasmic and nuclear targets. It is of interest that the chaperone Hsp27 (heat shock protein 27) associates with filaggrin in a phosphorylation-dependent

manner and that Hsp27 is a component of keratohyalin (O'Shaughnessy *et al.*, 2007).

We knocked down PND in the raft cultures of human keratinocytes by using an adenoviral siRNA approach. Mildner *et al.* (2010) knocked down filaggrin and observed loss of keratohyalin granules and impairment of lamellar body formation in human organotypic cultures. Reduction of glycine and serine content in CE from raft culture keratinocyte system infected with pAxewit2-PNDsiRNA may be due to reduced amount of loricrin in CE. This result strongly supports our chaperone hypothesis. The PND knockdown experiments in the raft cultures showed a reduction in loricrin protein levels but not K10. There may be other chaperones except PND for K10. The reason why loricrin mRNA was knocked down by the PND siRNA is not clear right now. There may be off-target effect by their siRNA. The molecular mechanism behind this observation is currently being analyzed in our laboratory.

In summary, this study shows that PND interacts with both loricrin and K10. Our results suggest that PND has a chaperone-like function similar to that of some other S100 proteins, and may play a role in the ordered assembly of the CE.

MATERIALS AND METHODS

Cell culture and nucleofection

The culture of HaCaT cells was carried out as previously described (Yoneda *et al.*, 2004). HaCaT cells were nucleofected using the Amaxa Cell Line Optimization Nucleofector Kit (Lonza, Walkersville, MD) (Han *et al.*, 2008). For nucleofection, 10 μg of loricrin in the pcDNA3.1/V5-His vector or pFLAG467proF plasmid was used (Presland *et al.*, 1997; Yoneda *et al.*, 2010a). Following trypsinization for 10 minutes, 4×10^6 cells were suspended in 100 μl of Cell Line Nucleofector Solution V in an Amaxa-certified cuvette. The solution was then pulsed with the appropriate program U-20. Immediately following pulsation, 500 μl of prewarmed DMEM was added to each cuvette. The cells were transferred to a 1.5-ml Eppendorf tube and incubated at 37 °C. After 10 minutes, the nucleofected cells were transferred to a 100-mm culture dishes containing fresh, prewarmed DMEM and maintained at 37 °C.

At 48 hours after nucleofection, cells were collected for further analysis. In each experiment, nucleofection efficiency was confirmed to be similar among different nucleofected plasmids using X-gal staining (Yoneda *et al.*, 2004).

Primary antibodies and reagents

The anti-V5 antibody was purchased from Life Technologies (Carlsbad, CA), the anti-cytokeratin 10 antibody from DAKO (Glostrup, Denmark), the mouse monoclonal anti-filaggrin (AKH1: sc-66192) from Santa Cruz Biotechnology (Santa Cruz, CA), and the mouse monoclonal anti-FALG (F1804) and the rabbit polyclonal anti-FLAG (F7425) antibodies from Sigma-Aldrich (St Louis, MO). The profilaggrin *N*-terminal antibodies A2 and B1 (to human profilaggrin) were previously described (Presland *et al.*, 1997; Pearton *et al.*, 2002). A peptide with the *N*-terminal 20 amino acids of human loricrin (SYQKKQPTPQPPVDCVKTSG) was synthesized. This peptide covalently coupled to keyhole limpet hemocyanin was used to immunize guinea pigs and mice. Guinea pig antiserum was affinity purified using a peptide affinity column. Mice were immunized intraperitoneally with the above immunogen. At 3 days after the final injection, the lymph nodes were removed and the lymphocytes were fused with mouse P3 myeloma cells. The clones that produced antibodies specifically recognized the human loricrin were expanded.

Loricrin knockout mice

We isolated the mouse loricrin gene from a 129/Sv mouse genomic library and made loricrin knockout mice as previously described (Koch *et al.*, 2000). To minimize phenotype variation due to the mixed (129/Sv and C57Bl/6) genetic background, we crossed the loricrin knockout mice into the FvB mouse strain. The experiments described in this paper were performed using mice from the eighth backcross.

Immunofluorescence microscopy

Normal human skin was obtained during plastic surgery procedures with informed consent using protocols approved by the local medical ethics committee that complies with the Declaration of Helsinki Principles. Immunostaining was performed as described previously (Yoneda *et al.*, 1990a, 2004).

Immunoelectron microscopy

Normal human skin was obtained during plastic surgery procedures with informed consent using protocols approved by the local medical ethics committee that complies with the Declaration of Helsinki Principles. Skin samples were taken from newborn loricrin$^{-/-}$ mice and diced with a scalpel into blocks of 1–2 mm square immediately after killing. These samples were immediately fixed and prepared for immunoelectron microscopy using LR White. Specimens were examined and images were recorded in a JEM-1200EX (JEOL, Akishima, Japan). Quantitative analysis was performed as described previously (Yoneda *et al.*, 1990b).

Mouse profilaggrin constructs and Y2H assays

The complete mouse profilaggrin *N*-terminus that was used as a bait for the Y2H screen was prepared by PCR (forward, 5′-CCCGAATTC TCCGCTCTCCTGGAAAGCATCACTAG-3′ and reverse, 5′-CCCGG ATCCTTACCTGGATCTCCTCTGGTCAGCC-3′) using a mouse profilaggrin cDNA clone as template. The PCR product was digested with the enzymes *Eco*RI and *Bam*HI (underlined in PCR primers) and cloned into pOBD, downstream and in-frame with the GAL4 DNA-binding domain. The individual mouse profilaggrin A domain (amino acids 1–99) and B domain (residues 99–283) constructs were prepared by PCR and cloned into pOBD, downstream and in-frame with the GAL4 DNA-binding domain. Individual human profilaggrin A and B domain comprised amino acids 1–98 and 99–293, respectively, expressed as GAL4 DNA-binding domain fusion proteins in pOBD. The p53 and SV40 T-antigen constructs were purchased from Clontech (Palo Alto, CA). The Y2H screens were performed with a mouse epidermal cDNA library prepared in the vector pGADT7 (obtained from Dr M Morasso, NIAMS, National Institutes of Health, Bethesda, MD) using the complete mouse profilaggrin *N*-terminus as bait. Plasmids were transformed into *Saccharomyces cerevisiae* strain PJ694A (Yeast Resource Center, University of Washington, Seattle, WA) using a commercial yeast transformation kit (Zymo Research, Orange, CA). For the screen,

$\sim 1 \times 10^6$ transformants were grown at 30 °C on 15-cm YPD plates lacking histidine, leucine, and typtophan and containing 2.5 mM 3-AT (Sigma-Aldrich). Positive clones were rescued from yeast by first growing on leucine-deficient plates and then in YPDA media to isolate plasmid DNA (Zymoprep, Zymo Research). Plasmid DNA was transformed into competent MH4 *E. coli* cells and miniprep DNA isolated from 1–3 individual colonies for restriction digestion and DNA sequencing. The identity of each cDNA clone was determined by BLAST (Basic Local Alignment Search Tool, Bethesda, MD) searches of the NCBI (National Center for Biotechnology Information) database. Only cDNAs that were in-frame with upstream GAL4 activation domain of pGADT7 were further considered.

Further analyses ("retests") of each positive clone was performed against the profilaggrin *N*-terminus (also individual A and B domain constructs) and a panel of negative controls including a series of *S. cerevisiae* cDNAs (ASK, DAD4, DUO1, NDC80, RAD17, SWN1; provided by Dr S Fields, University of Washington), human S100A2, and human p53 (Hudson *et al.*, 1997). These results were generally done with histidine, leucine, and typtophan plates containing 2.5–20 mM 3-AT.

Immunoprecipitation and immunoblot analysis

Immunoprecipitation and immunoblot analysis was performed as described previously (Yoneda *et al.*, 2004). The proteins were detected using an enhanced chemiluminescence system (GE Healthcare Bio-Biosciences, Piscataway, NJ) according to the manufacturer's instructions.

GST pull-down

GST-PND was coupled to glutathione agarose (GE Healthcare Bio-Biosciences) according to the manufacturer's instructions, and cell extract was added and incubated for 2 hours at 4 °C. Proteins were eluted in SDS-PAGE buffer and analyzed by immunoblot analysis.

Preparation of the recombinant adenoviral vectors

The target sequences for PND siRNA oligonucleotides were designed by siRNA Design Support System (Takara Bio, Otsu, Japan) (Miyake *et al.*, 1996; Dai *et al.*, 2010). The oligonucleotide containing the siRNA target sequence for human PND (5′-CTATGACACCACTGATAGT-3′) and the appropriate restriction sites was synthesized and inserted into pBAsi-hU6 Neo (Takara Bio). This vector was designated as pBAsi-hU6 Neo PNDsiRNA. Control vector was constructed through the same procedure using a scrambled sequence (5′-GATCCGTCTTAATCGCGTATAAGGCTAGTGCT CCTGGTTGGCCTTATACGCGATTAAGACTTTTTTA-3′), which has a nucleotide composition close to that of the PND target sequence. A fragment containing the H1 promoter and the inserted sequence (H1 promoter-PND) was then excised by *Eco*RV digestion and ligated into the pAxcwit2 vector. For production of adenoviruses, the packaging cell line (human embryonic kidney (HEK) 293 cells) was maintained in DMEM supplemented with 10% fetal bovine serum and the appropriate antibiotics. At 1 day before transfection, cells were seeded onto plates containing 4×10^6 cells per plate and incubated in an atmosphere of 5% CO_2 at 37 °C. pAxewit2-PNDsiRNA and pAxewit2 vector of scrambled sequence were linearized with BspT104I and transfected into the cells using TransIT-293 (Takara Bio) according to the protocol. At 6 hours after transfection, fresh growth medium was added to the cells. After 1 day, the cells were spread in three 96-well plates in a 10-fold serial dilution mixed with untransfected HEK293 cells. After being maintained in culture for 10–15 days, virus clones were isolated and propagated further to assess restriction analysis. The method used to propagate adenovirus was as described (Miyake *et al.*, 1996). The raft culture keratinocyte system was constructed according to Mildner *et al.* (2010).

Quantitative real-time reverse-transcriptase–PCR

Total RNA was isolated from control raft cultured keratinocyte and raft cultured keratinocyte infected with pAxewit2-PNDsiRNA using FastPure RNA Kit (Takara Bio). For reverse transcription, 25 ng of total RNA from each sample was used as a template in a 10 µl reaction system containing random primers and PrimeScript RT Enzyme Mix I (Takara Bio). Reverse transcription reactions were conducted at 37 °C for 15 minutes and then inactivated at 95 °C for 5 minutes. Quantitative real-time PCR was performed using one step SYBR PrimeScript RT-PCR Kit II (Perfect Real Time). The reaction volume was 25 µl, which included cDNA and SYBR Premix Ex Taq (Takara Bio) as well as 10 µM PCR forward primer and 10 µM PCR reverse primer. Reactions were performed at 95 °C for 10 seconds followed by 40 cycles at 95 °C for 5 seconds and 60 °C for 30 seconds. Each experiment was repeated two times. Glyceraldehyde-3-phosphate dehydrogenase was used as an internal control for the relative quantification of target genes using the comparative threshold cycle method.

CONFLICT OF INTEREST

The authors state no conflict of interest.

ACKNOWLEDGMENTS

We are grateful to T Moriue and K Nakai for insightful discussions during the course of this study. We are also grateful to Dr N Fusenig for HaCaT cells; F Naruse, T Takamura, and M Kato for technical assistance and artwork. This work was in part supported by research grants from the Ministry of Education, Culture, Sports and Technology of Japan (Kiban C, 18591250 to KY) and by grant R01 AR49183 from the National Institutes of Health (to RBP). The costs of publication of this article were defrayed in part by the payment of page charges. This article must therefore be hereby marked "advertisement" in accordance with 18 U.S.C. Section 1734 solely to indicate this fact.

SUPPLEMENTARY MATERIAL

Supplementary material is linked to the online version of the paper at http://www.nature.com/jid

REFERENCES

Albers K, Fuchs E (1989) Expression of mutant keratin cDNAs in epithelial cells reveals possible mechanisms for initiation and assembly of intermediate filaments. *J Cell Biol* 108:1477–93

Backendorf C, Hohl D (1992) A common origin for cornified envelope proteins? *Nat Genet* 2:91

Broome AM, Ryan D, Eckert RL (2003) S100 protein subcellular localization during epidermal differentiation and psoriasis. *J Histochem Cytochem* 51:675–85

Candi E, Schmidt R, Melino G (2005) The cornified envelope: a model of cell death in the skin. *Nat Rev Mol Cell Biol* 6:328–40

Dai W, He W, Shang G *et al.* (2010) Gene silencing of myofibrillogenesis regulator-1 by adenovirus-delivered small interfering RNA suppresses cardiac hypertrophy induced by angiotensin II in mice. *Am J Physiol Heart Circ Physiol* 299:H1468–75

Dale BA, Presland RB, Lewis SP *et al.* (1997) Transient expression of epidermal filaggrin in cultured cells causes collapse of intermediate